Method of electrochemical etching of tungsten tips with controllable profiles

Cite as: Rev. Sci. Instrum. **83**, 083704 (2012); https://doi.org/10.1063/1.4745394
Submitted: 18 May 2012 . Accepted: 27 July 2012 . Published Online: 15 August 2012

Wei-Tse Chang, Ing-Shouh Hwang, Mu-Tung Chang, Chung-Yueh Lin, Wei-Hao Hsu, and Jin-Long Hou

Method of electrochemical etching of tungsten tips with controllable profiles

Wei-Tse Chang,[1] Ing-Shouh Hwang,[1,a)] Mu-Tung Chang,[1] Chung-Yueh Lin,[1,2] Wei-Hao Hsu,[1,3] and Jin-Long Hou[1,4]
[1]*Institute of Physics, Academia Sinica, Nankang, Taipei 11529, Taiwan*
[2]*Department of Physics, National Taiwan University, Taipei 10617, Taiwan*
[3]*Department of Materials Science and Engineering, National Tsing Hua University, Hsinchu 30013, Taiwan*
[4]*Department of Physics, National Taiwan Normal University, Taipei 11677, Taiwan*

(Received 18 May 2012; accepted 27 July 2012; published online 15 August 2012)

We demonstrate a new and simple process to fabricate tungsten tips with good control of the tip profile. In this process, we use a commercial function generator without any electronic cutoff circuit or complex mechanical setup. The tip length can be varied from 160 μm to 10 mm, corresponding to an aspect ratio of 1.6–100. The radius of curvature of the tip apex can be controlled to a size $<$10 nm. Surface roughness and the taper angle can be controlled independently. Through control of the etching parameters, the tip length, the radius of curvature, surface roughness, and the taper angle can be controlled to suit different requirements of various applications. The possible etching mechanisms are also discussed. © *2012 American Institute of Physics*. [http://dx.doi.org/10.1063/1.4745394]

I. INTRODUCTION

Sharp metal tips have been used in a wide variety of technical applications, including the probes in scanning probe microscopy (SPM),[1,2] emitters of electron,[3] or ion beams,[4,5] point contacts in conductance measurements,[6] etc. Tungsten is a favorite material for fabricating a sharp tip because of its high mechanical strength and highest melting point. In addition, tungsten tips can be etched through simple electrochemical methods. However, different applications may have different requirements for the tip profile. For example, a small radius of curvature (ROC) at the tip apex is good for probes used in SPM. In the multi-probe measurements of surface conductance on nano-structures, it is often desirable to use long and skinny tips as the probes because they allow placing probes close to one another. Even though tips with a smooth surface are usually adequate for most applications, the liquid-metal ion source emitter requires a tungsten tip with a rough surface[7] and a large taper angle.[8] Therefore, it would be very useful to develop techniques to fabricate a tungsten tip with a desired geometry.

Tungsten tips are typically fabricated with direct current (dc) etching. In 1990, Ibe *et al.* proposed a method of dc etching for fabrication of tungsten tips with a ROC of $\sim$30 nm by employing an electronic cutoff circuit.[1] This is because a faster cutoff time yields a sharper tip. Later, several researchers proposed electronic circuits to reduce the cutoff time.[9–13] Modification of the tip length was also demonstrated by applying different dc voltages[10] or by changing the height of a hollow cylinder cathode.[14] Alternating current (ac) etching can also be applied for the tip fabrication, but it is usually more difficult to control than dc etching.[15]

Recently, Ju *et al.*[16] proposed an electrochemical etching method in which the neck-in position of a tungsten wire could be adjusted mechanically with a precision motorized stage. In combination with a DSP-based control unit, the tip length, ROC, and the cone angle can be controlled. However, this approach requires complicated mechanical and electronic control setups. In addition, it is not clear how each parameter of the tip profile can be independently controlled.

In this study, we present a simple, inexpensive, and flexible process to produce tungsten tips with a controllable tip profile. Neither a complicated mechanical setup nor an electronic cutoff circuit is required. A commercial function generator is employed to fabricate tungsten tips with a desired profile by controlling the dc etching potential, dc etching duration, the pulsed potentials, the pulse width, etc. The possible etching mechanisms and the evolution of the tip profile are discussed in this paper.

II. EXPERIMENTAL PROCEDURES

Figure 1(a) shows a schematic of the experimental setup. A tungsten wire (anode, diameter of 0.1 mm) is placed inside a tungsten wire loop (cathode, diameter of 0.15 mm). A 10 M potassium hydroxide solution (KOH) is used as an electrolyte for tungsten etching. There are two main reasons for using KOH electrolyte with such a high concentration. One is to reduce the process time due to an enhanced etching rate and the other is to make the meniscus stable at the air/electrolyte interface during the etching process. At low electrolyte concentrations, the meniscus is often fluctuating during etching, which renders the profile control difficult.

Figure 1(b) shows a schematic of the applied potential generated from a commercial function generator (AFG-3051, GW Instek, Taiwan), which is composed of a dc etching potential followed by two stages of pulses, as shown in Figure 1(b). The maximum output current of the function generator is 200 mA, which is significantly larger than the current required for the tip etching presented in this work

a)E-mail: ishwang@phys.sinica.edu.tw, Tel.: +886-2-2789-6764, FAX: +886-2-2783-4187.

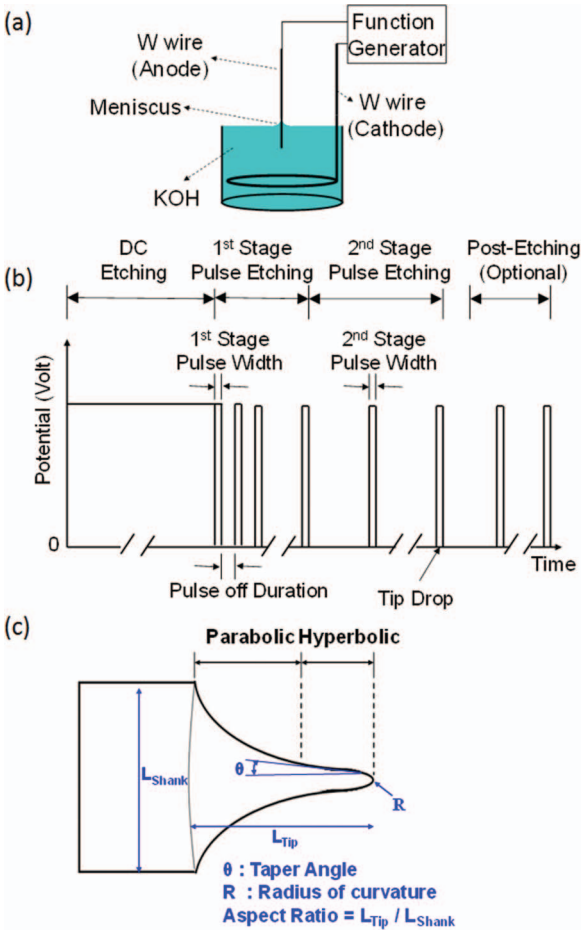

FIG. 1. Schematic diagrams of (a) the experimental setup, (b) the applied potential, and (c) the definition of the tip profile. (a) The experimental setup including KOH electrolyte, tungsten wires with diameter of 0.1 mm/0.15 mm as anode/cathode and a commercial function generator as power supply. (b) The applied potential composed of dc and subsequent pulse potentials. (c) Tip profile includes tip length, radius of curvature at apex, and taper angle.

(<20 mA). A duration of a dc etching potential is first applied to the tungsten wire, which results in non-uniform etching with the fastest reaction rate occurring at a depth slightly below the air-electrolyte interface.[17] A necking shape with a narrowest region in the wire appears after a short period of dc etching. If a dc potential is applied continuously, the necking part would become so thin that the bottom part of the tungsten wire drops eventually. Two separate wire parts with a sharp tip at an end of each part are created. Usually the lower part is discarded. Here we carefully control the duration of the dc etching. The first-stage pulses, with the pulse-off duration of 100 ms and the pulse-on duration of 1 ms, are applied for further etching. When the necking part of the wire decreases to a diameter below 10 μm, which can be viewed with an optical microscope, the second-stage pulses are applied until the necking part of the wire breaks off. We note that this diameter is not very critical. If the second-stage pulses are applied when the necking diameter is larger than 10 μm, the duration of second-stage pulses will need to be prolonged for the break-off to occur. The second-stage pulses typically have the pulse-on duration ranging from 1 to 100 ms and the pulse-off duration set to a longer time, say 1 s, for human response to turn off the pulses right after the lower part of the wire breaks off. The last pulse allows us to control the tip radius during the break-off, similar to the effect of typical electronic cutoff circuits. We may also add post-etching pulses with the pulse width of 1 ms for further control of the tip apex. Even though the dc etching potential and the pulse etching potential can be independently adjusted, we tend to use the same potential for both dc etching and pulse etching, which can be varied from 2 V to 6 V. The definition of the tip geometry is illustrated in Figure 1(c). The front part of the tip has a hyperbolic shape and the rear part has a parabolic shape. The taper angle is defined in the hyperbolic region. The aspect ratio is defined as the ratio of the tip length (L_{Tip}) to the shank diameter (L_{Shank}). Through careful control of the dc etching potential, the dc etching duration, the first-stage pulse width, the second-stage pulse width, and the number of post-etching pulses, we can control several parameters of the tungsten tip profile, including the tip length, the ROC, the surface roughness, and the taper angle.

III. RESULTS AND DISCUSSION

We find that the tip surface roughness can be controlled by changing the dc etching potential. Figures 2(a)–2(e) show scanning electron microscope (SEM) images of tungsten tips etched under the potential of 2 V, 3 V, 4 V, 5 V, and 6 V, respectively. The corresponding dc etching duration is varied for the formation of a similar necking shape on the immersed tungsten wires at different potentials. The pulse width of both the 1st stage pulses and the 2nd stage pulses are 1 ms. The

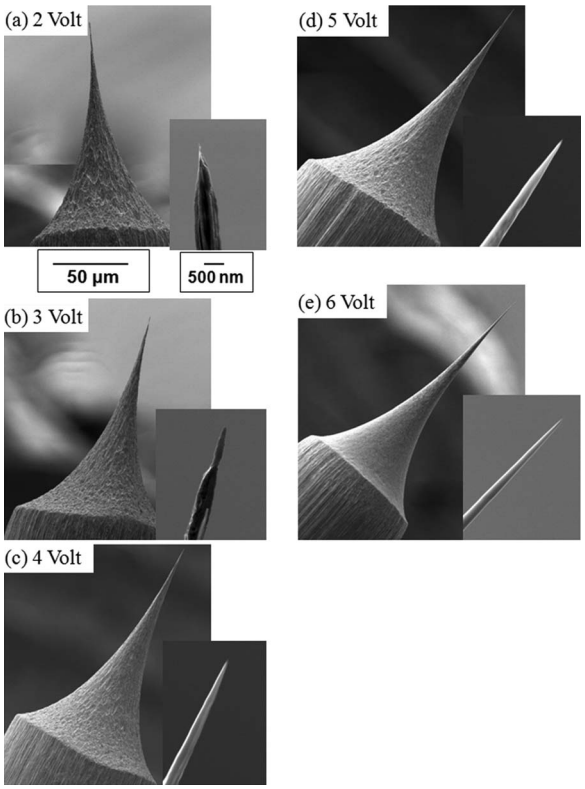

FIG. 2. (a)–(e) show SEM images of tungsten tips etched with the potential of 2 V, 3 V, 4V, 5V, and 6V, respectively. Clearly, surface roughness decreases with increasing applied potential.

TABLE I. The etching parameters for tip profile control.

Corresponding figures	dc		Pulse width		Number of post-etching pulses
	Volt (V)	Duration (s)	1st stage pulse (ms)	2nd stage pulse (ms)	
Reference condition Figs. 2(e)/3(b)/4(b)	6	20	1	1	0
Figure 2(a)	2	40	1	1	0
Figure 2(b)	3	35	1	1	0
Figure 2(c)	4	30	1	1	0
Figure 2(d)	5	25	1	1	0
Figure 3(c)	6	10	1	1	0
Figure 3(d)	6	5	1	1	0
Figure 3(e)	6	0	1	None	0
Figure 4(c)	6	20	1	10	0
Figure 4(d)	6	20	1	50	0
Figure 4(e)	6	20	1	70	0
Figure 4(f)	6	20	1	100	0
Figure 5(b)	6	20	1	1	1
Figure 5(c)	6	20	1	1	2
Figure 5(d)	6	20	1	1	3
Figure 5(e)	6	20	1	1	4

etching parameters are listed in Table I. Clearly, a lower potential yields a rougher tip surface. The roughest surface is observed in Figure 2(a) for etching at 2 V. The tip surface becomes smoother when the applied potential is increased, as shown in Figures 2(b)–2(e). In previous studies using dc etching, similar trend between the tip surface roughness and the dc potential was reported.[14–16,18]

There are several etching parameters, including the dc etching duration, the etching potential, the first-stage pulse width, the second-stage pulse width, and the number of post-etching pulses. Here, we choose a typical etching condition as a reference and only one etching parameter is changed each time to find the effect on a certain parameter of the tip profile. The reference condition is listed in Table I, which also includes all etching parameters for the images shown in this paper. Note that the tips shown in Figures 2(e), 3(b), and 4(b) are etched with the reference condition.

Figure 3(a) shows the effect of various etching parameters on the tip length. Apparently, the dc etching duration is the most effective parameter for tuning the tip length, and the tip length decreases with increasing dc etching duration. By changing this parameter, a wide range of the tip length, from 162 to 1260 μm, can be obtained, as shown in Figures 3(b)–3(e). Clearly, the maximum tip length is obtained if no dc etching is used (i.e., the dc etching duration is zero). At this condition, the tip length is nearly the same as the immersion length of the tungsten wire prior to etching. The immersion lengths for the cases in Figures 3(b)–3(e) are ~1.3 mm. To increase the tip length, we have also extended the immersion length to 10 mm and the tip length of ~10 mm is obtained, as shown in Figure 3(f). At such a high aspect ratio (~100), the tip has a diameter of 4 ± 2 μm, which may be used as a thin metal wire for some applications, such as a biprism for charged particle beams. Notice that the parabolic necking, which is typically observed for dc etching, is not seen in Figures 3(e) and 3(f).

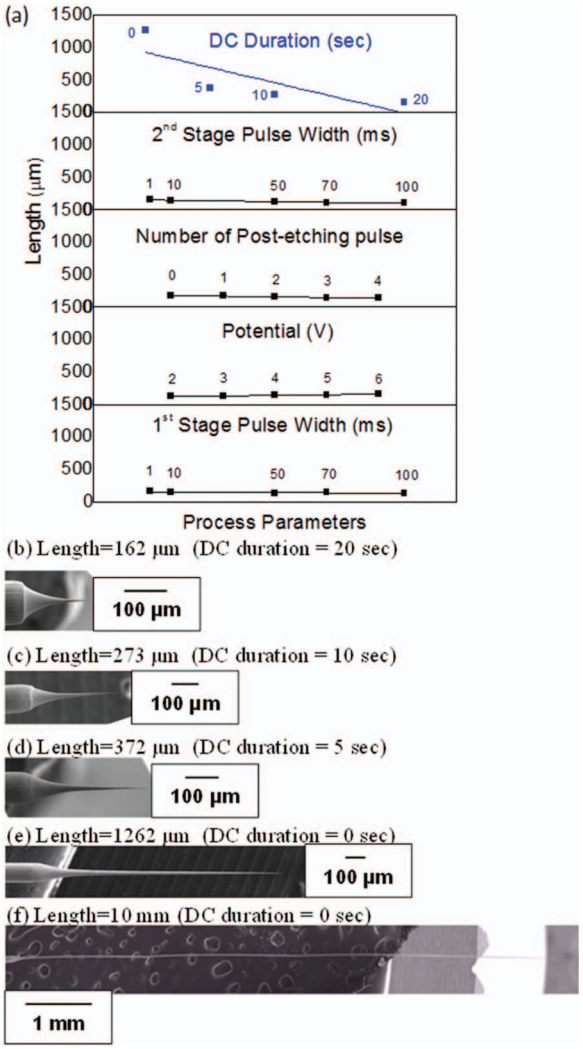

FIG. 3. (a) shows relationship between the tip length and various etching parameters. (b)–(f) show SEM images of tungsten tips with different lengths controlled by the dc duration.

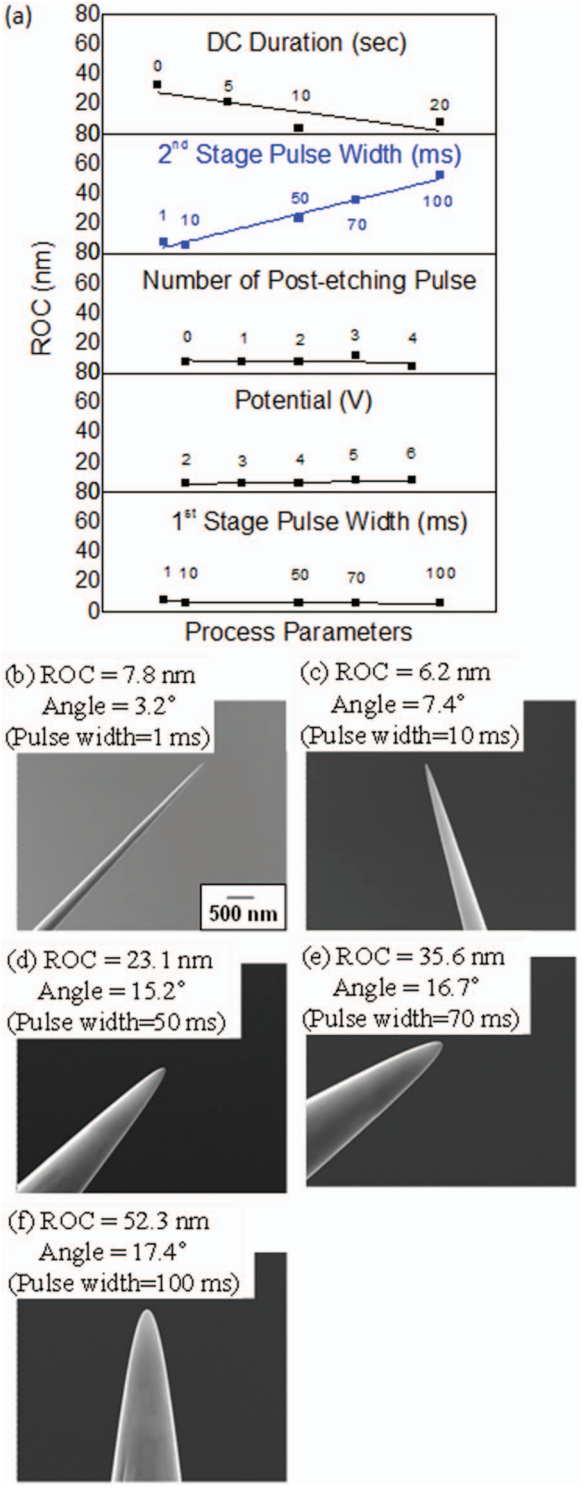

FIG. 4. (a) The effect of various etching parameters on ROC. (b)–(f) show tungsten tips with different ROCs controlled by the 2nd stage pulse width.

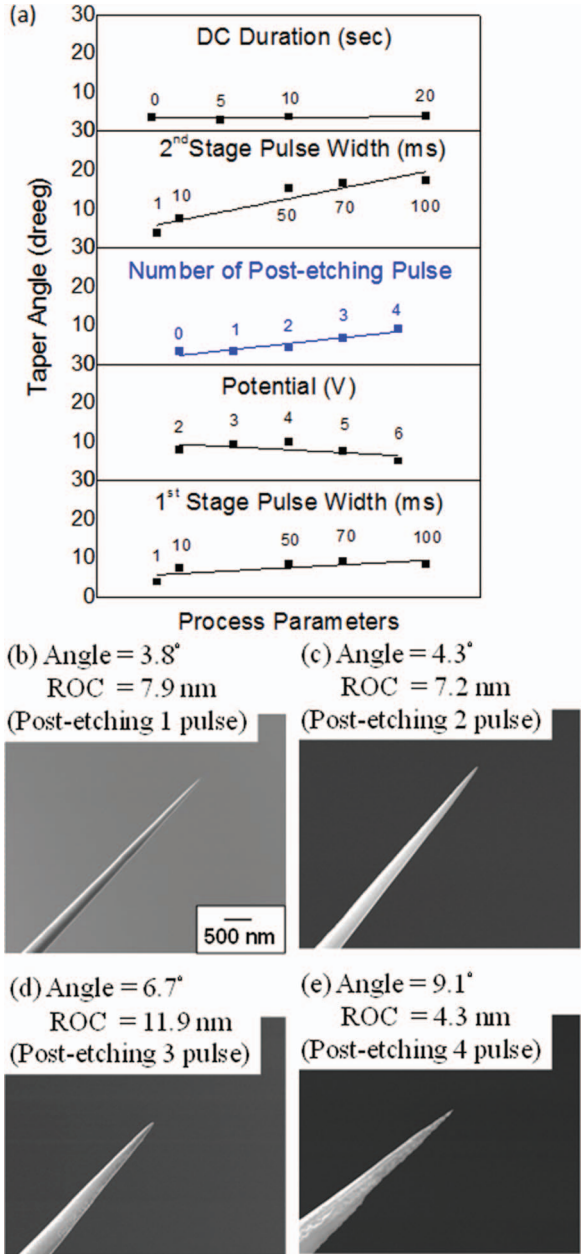

FIG. 5. (a) illustrates the relationship between the taper angle and various etching parameters. (b)–(e) show the tungsten tips with different taper angles controlled by the number of post-etching pulses. The pulse width is 1 ms.

Figure 4(a) shows the effects of various etching parameters on the tip radius. We find that the ROC can be tuned by the pulse width of the 2nd stage pulses. As the pulse width increases from 1 ms to 100 ms, the corresponding ROC varies from 7.8 nm to 52.3 nm, as shown in Figures 4(b)–4(f). Note that the tip shown in Figure 4(b) is prepared with the reference condition and the tips shown in Figures 4(c)–4(f) have the same etching parameters except for the pulse width of the second-stage pulses. In addition, the dc etching duration also affects the ROC value. A longer duration yields a sharper tip apex.

Figure 5(a) shows the relationship between the taper angle and various etching parameters. The number of post-etching pulses and the pulse width of the second-stage pulses both have significant effects on the taper angle. The effect of the former parameter is shown in Figures 5(b)–5(e). The taper angle is 3.8°, 4.3°, 6.7°, to 9.1° for 1, 2, 3, and 4 post-etching pulses, respectively, and the ROC is kept within the range of 7.8 ± 3.1 nm. The effect of the later etching parameters on the taper angle can be seen in Figures 4(b)–4(f). However, the ROC is also altered by this parameter.

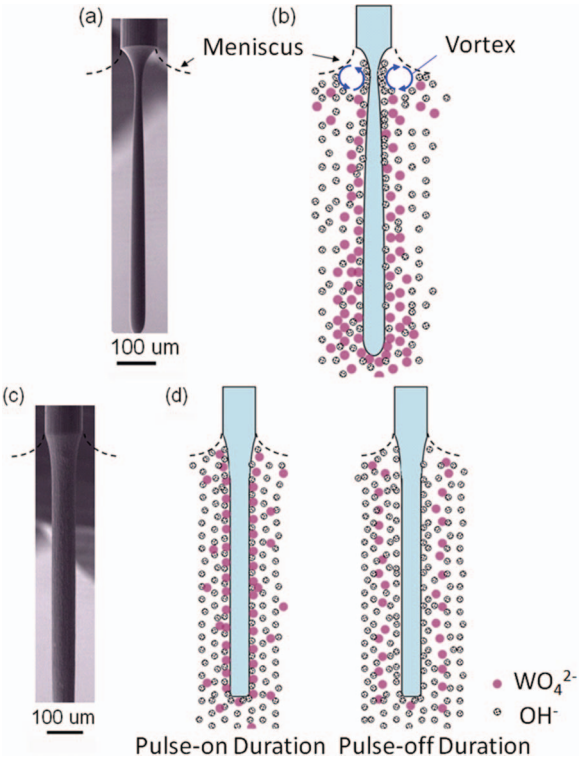

FIG. 6. Schematic diagrams of anion distribution under (a) and (b) dc and (c) and (d) pulse etching and the corresponding SEM images.

We have carried out further experiments to understand the etching mechanism. Figure 6(a) shows a SEM image of a tungsten wire after etching at dc 2 V for 50 s. A necking shape is typically observed just below the meniscus, indicating a non-uniform etching rate along the tungsten wire. This is probably due to the non-uniform concentration of OH^- ions along the wire immersed in the electrolyte. The concentration near the top of the meniscus is lower than that of the bulk solution probably due to insufficient mass transfer of OH^- ions. In addition, the etching also produces soluble tungstate anions (WO_4^{2-}), which form a viscous flow down along the wire surface[1] and gradually accumulate at the lower part of the wire. The tungstate decreases the activity of OH^- ion and the current density of reaction is also dependent on the activity and concentration of OH^- ions.[14] A vortex formed below the meniscus has been proposed.[17] This flow splitting removes the reaction products at the wire neck and the variation in the electrochemical reaction rates is caused by the gradient of the tungstate thickness, as illustrated in Figure 6(b). As the etching continues, the necking part becomes thinner and thinner and eventually the lower part of the wire breaks off. A sharp tip is thus formed at the necking part.

In contrast, a uniform etching is seen when using the pulsed potential and no necking is observed, as shown in Figure 6(c). This may be related to the pulse-on and pulse-off cycle of the potential applied on the tungsten wire. As proposed in the illustration shown in Figure 6(d), tungstate anions are attracted to the positive potential of the wire during the pulse-on duration and may desorb from the tungsten surface and dissolved into nearby solution in the pulse-off duration. Since tungstate anions do not accumulate to form a viscous flow along the wire, the concentration of OH^- ions is more uniformly distributed along the entire wire in solution, except for the part in the meniscus. This leads to a uniform etching of the wire. In fact, this etching pattern is very similar to the ac etching of tungsten wires probably because of the similar behavior of anions near the anode. Thus, we think our first-stage pulse etching may be replaced by the ac etching. Just typical ac etching methods have no good control at the moment the tip breaks off at the necking part.

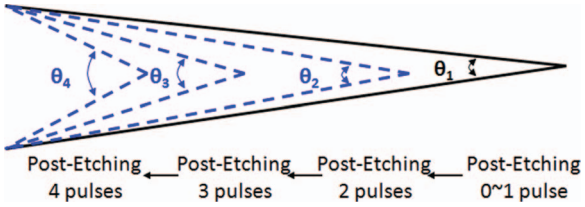

FIG. 7. Schematic diagram proposed for the effect of post-etching pulses. The taper angle increases with increasing post-etching pulses and the tip length is shortened slightly.

In our etching method, we combine both the dc etching and the pulse etching (or ac etching). The initial dc etching is used to control the formation of the necking part, which allows us to control the position of the break-off point, i.e., the final tip length. The pulse etching allows us to control other parameters of the tip profile. For example, the second-stage pulse width lets us control the tip radius. In the typical dc etching, a tip with ROC of 10–30 nm can be obtained with a fast cutoff time in the ns scale.[1,8–13] Here, we can control the ROC with the pulse width in the ms scale, indicating that the pulse width in the pulse etching is more effective than the cut-off time in the dc etching for controlling the ROC. This is probably related to the very fast etching rate at the necking part during the dc etching. The tip apex might become blunt easily at the moment that the necking part breaks off, and thus a sharp cut-off circuit is required. For the pulse etching, the uniform etching suggests a much lower current density at the tip apex.

Figure 7 illustrates the evolution of the tip apex under post-etching pulses. The taper angle increases ($\theta_1 < \theta_2 < \theta_3 < \theta_4$) with increasing number of the post-etching pulses, but the corresponding tip length decreases only slightly. The ROCs might be maintained after application of a small number of post-etching pulses due to the evenly distributed anion in the pulse etching.

IV. CONCLUSIONS

Profile control of tungsten tips is desirable for many different applications. Here, we propose a simple and reliable electrochemical method to fabricate tungsten tips with good control of the tip profile. Tips with the apex radius smaller than 10 nm or with a length longer than 1 mm can be reliably prepared.

ACKNOWLEDGMENTS

This work is supported by Academia Sinica (AS-99-TP-A02) of ROC.

[1]J. P. Ibe, P. P. Bey, Jr., S. L. Brandow, R. A. Brizzolara, N. A. Burnham, D. P. DiLella, K. P. Lee, C. R. K. Marrian, and R. J. Colton, J. Vac. Sci. Technol. A **8**, 3570 (1990).
[2]G. Binnig, H. Rohrer, Ch. Gerber, and E. Weibel, Phys. Rev. Lett. **49**, 57 (1982).
[3]P. B. Hirsch, A. Howie, R. B. Nicholson, D. W. Pashley, and M. J. Whelan, *Electron Microscopy of Thin Crystals*, 1st ed. (Butterworths London, 1965).
[4]T. T. Tsong, *In Atom-Probe Field Ion Microscopy* (Cambridge University Press, Cambridge, England, 1990).
[5]H. S. Kuo, I. S. Hwang, T. Y. Fu, J. Y. Wu, C. C. Chang, and T. T. Tsong, Nano Lett. **4**, 2379 (2004).
[6]A. S. Walton, C. S. Allen, K. Critchley, M. L. Gorzny, J. E. M. Kendry, R. M. D. Brydson, B. J. Hickey, and S. D. Evans, Nanotechnology **18**, 065204 (2007).
[7]A. Wagner and T. M. Hall, J. Vac. Sci. Technol. **16**, 1871 (1979).
[8]A. E. Bell and L. W. Swanson, Appl. Phys. A **41**, 335 (1986).
[9]A. I. Oliva, A. R. Romero, and J. L. Pena, Rev. Sci. Instrum. **67**, 1917 (1996).
[10]D. I. Kim and H. S. Ahn, Rev. Sci. Instrum. **73**, 1337 (2002).
[11]F. Bastiman, A. G. Cullis, and M. Hopkinson, J. Vac. Sci. Technol. B **28**, 371 (2010).
[12]L. Anwei, H. Xiaotang, L. Wenhui, and J. Guijun, Rev. Sci. Instrum. **68**, 3811 (1997).
[13]Y. Nakamura, Y. Mera, and K. Maeda, Rev. Sci. Instrum. **70**, 3373 (1999).
[14]W. X. Sun, Z. X. Shen, F. C. Cheong, G. Y. Yu, K. Y. Lim, and J. Y. Lin, Rev. Sci. Instrum. **73**, 2942 (2002).
[15]S. L. Toh, H. Tan, J. C. Lam, L. C. Hsia, and Z. H. Mai, J. Electrochem. Soc. **157**, E6 (2010).
[16]B. F. Ju, Y. L. Chen, and Y. Ge, Rev. Sci. Instrum. **82**, 013707 (2011).
[17]M. Kulakov, I. Luzinov, and K. G. Kornev, Langmuir **25**, 4462 (2009).
[18]D. Xu, K. M. Liechti, and K. Ravi-Chandar, Rev. Sci. Instrum. **78**, 073707 (2007).